arXiv:astro-ph/9809323v1 24 Sep 1998

Star formation in clusters: a survey of compact mm-wave sources in the Serpens core

Leonardo Testi and Anneila I. Sargent
Division of Physics, Mathematics and Astronomy, California Institute of Technology, MS 105-24, Pasadena, CA 91125 (lt@astro.caltech.edu,afs@astro.caltech.edu)

ABSTRACT

We report the results of a millimeter interferometric survey of compact 3 mm continuum sources in the inner $5.5' \times 5.5'$ region of the Serpens core. We detect 32 discrete sources above 4.0 mJy/beam, 21 of which are new detections at millimeter wavelengths. By comparing our data with published infrared surveys, we estimate that 26 sources are probably protostellar condensations and derive their mass assuming optically thin thermal emission from dust grains. The mass spectrum of the clumps, $dN/dM \sim M^{-2.1}$, is consistent with the stellar initial mass function, supporting the idea that the stellar masses in young clusters are determined by the fragmentation of turbulent cloud cores.

Subject headings: ISM: clouds – ISM: radio continuum – stars: formation

1. Introduction

The theory of isolated star formation is in general fairly well understood (e.g. Shu et al. 1987). One notable flaw, however, is its failure to predict the resulting stellar masses. Stars in the field are known to be distributed according to a well defined mass function (e.g. Salpeter 1955; Kroupa, Tout & Gilmore 1993), and a complete theory of star formation must be able to predict this mass distribution, the Initial Mass Function (IMF). On the other hand, it seems very likely that most stars form in clusters rather than in isolation (Lada 1992; Zinnecker, McCaughrean & Wilking 1993; Lada, Alves & Lada 1996; Testi, Palla & Natta 1998). Thus any understanding of the star formation process must also be closely related to the way in which the IMF originates in clusters. Indeed, young embedded clusters appear to be populated by stars with a mass distribution very close to that observed in the solar neighbourhood (Hillenbrand 1997; Lada et al. 1996).

The IMF may result naturally from the protostellar accretion process. Adams & Fatuzzo (1996), for example, suggest outflow/inflow interactions as the mechanism that

determines stellar masses. Alternatively, the stellar mass distribution may be caused by the fragmentation process in turbulent, cluster-forming, dense cores (Myers 1998; Klessen, Burkert & Bate 1998). If the fragmentation hypothesis is correct, the prestellar condensations in cluster-forming molecular cores should be very close to the IMF of the stars in young embedded clusters and in the field. Interferometric molecular line studies of cloud cores (Pratap, Batrla & Snyder 1990; Kitamura, Kawabe & Ishiguro 1992) yield contradictory results, depending on the chemical and physical conditions assumed for the emitting gas. Observational evidence supporting the fragmentation origin of the IMF has been obtained by Motte, André & Neri (1998), in 1.3 mm continuum maps of ρ-Ophiuchi, a cluster forming core, using the IRAM 30-m telescope. The mass spectrum of the prestellar and protostellar clumps within the core appear consistent with the IMF. Surveys of additional cluster-forming molecular cores are needed to confirm that this result holds generally and to constrain the theoretical models.

At the angular resolution achievable with the IRAM-30m/bolometer system at 1.3 mm, $\sim 13''$, it is possible to probe detailed cloud core structure only in the star forming regions closest to the Sun, such as Taurus or Ophiuchus. Millimeter wavelength interferometers, however, offer both high spatial resolution and high sensitivity, and at these wavelengths the dust emission is probably optically thin, allowing a reasonable estimate of clump masses. Moreover, thanks to the interferometric filtering capability, smooth, extended emission from the molecular cloud core in which clumps are embedded is resolved out. Using the Owens Valley Radio Observatory (OVRO) millimeter array, we have begun a program of high resolution, millimeter-wave mapping of molecular cloud cores with a view to establishing whether the prestellar clump mass function and the IMF are in general similar. In addition to the above-mentioned advantages, the OVRO array enables simultaneous observation of molecular line and broad band continuum emission. Any contamination of the continuum flux by molecular line radiation can therefore be eliminated, allowing more accurate mass estimates. The results of this program should constrain theoretical models of the IMF.

Here we present our results for the Serpens star-forming core (Loren et al. 1979; Ungerechts & Güsten 1984; White et al. 1995). At a distance of 310 pc (de Lara et al. 1991), and with an angular extent of few arcmin, this is an ideal target to search for compact prestellar and protostellar condensations. Inside the 1500 $M_\odot$ core is a young stellar cluster of approximate mass 15-40 $M_\odot$ (Strom, Grasdalen & Strom 1976; Eiroa & Casali 1992; Giovannetti et al. 1998). In addition, far-infrared and submillimeter observations reveal the presence of a new generation of embedded objects (Casali et al. 1993, hereafter CED; Hurt & Barsony 1996). The improved sensitivity and resolution over the large area, $\sim 5.5' \times 5.5'$, covered by our survey have enabled us to detect a large number of new mm sources and to derive the mass spectrum of the dust condensations.

2. Observations and results

We observed the $\sim 5.5' \times 5.5'$ inner region of the Serpens molecular core with the OVRO millimeter wave array during the period September 1997 – February 1998. The final map resulted from 50 separate pointings of the telescope during each transit. The primary beam size at 99 GHz is $\sim 73''$ (FWHM) and pointing centers were spaced by $\sim 42''$. Four configurations of the six 10.4-m dishes provided baselines in the range $\sim 5 - 80$ kλ. This (u, v) sampling ensures good sensitivity up to spatial scales of $\sim 30''$ equivalent to 0.045 pc, or 9300 AU, at the distance of Serpens. All telescopes are equipped with cryogenically cooled SIS receivers which provided average system temperatures of ~ 350 K (SSB) at the observing frequency. Continuum observations centered at 99 GHz were made in both (USB and LSB) 1 GHz wide bands of the analog correlator. An 8 MHz wide band at 0.125 MHz resolution of the digital correlator was centered on the CS(2–1) transition at 97.981 GHz at the Serpens core velocity, $v_{LSR} = 8.0$ km/s. Gain and phase were calibrated through frequent observations of the quasar 1741−038. 3C273 and/or 3C454.3 were used for passband calibration. The flux density scale was determined by observing Neptune and Uranus and the estimated uncertainty is less than 20%. All calibration and editing of the raw data have been performed with the MMA software package (Scoville et al. 1993). The NRAO–AIPS package was used for mapping and analysis.

To produce the final mosaic image of the region, we applied the AIPS VTESS task, which performs a simultaneous Maximum Entropy (MEM) deconvolution of all the observed pointings. We used natural weighting and applied gaussian tapering to the (u, v) data before mapping/deconvolution. Nevertheless, due to residual phase errors and strong dirty beam sidelobes, it was necessary to remove the three brightest point sources (SMM1, SMM3 and SMM4) before deconvolution. The final hybrid image of the observed region, shown in Fig. 1, was then obtained by restoring to the MEM mosaic the three clean images (obtained with the task IMAGR) of the bright sources. The synthesized beam is $5\farcs5 \times 4\farcs3$ FWHM, corresponding to linear resolution ~ 0.0075 pc, or 1500 AU, and the noise level is ~ 0.9 mJy/beam. The CS(2–1) data was used to produce a map of the integrated line emission and we verified that line contamination in our continuum map is negligible. Detailed analysis of the CS data goes beyond the scope of the present paper and will be presented separately.

3. Analysis

The angular resolution of the 99 GHz hybrid mosaic of the Serpens core region shown in Fig. 1 is a factor of 4 higher than that of the CED sub-millimeter map of the same region.

The sensitivity is more than 10 times higher than in the less extensive 3 mm continuum map of McMullin et al. (1994). The known far-infrared and sub-millimeter young stellar objects (CED; Hurt & Barsony 1996) are indicated by crosses, although their positional uncertainties are rather large. A particularly notable case is S68N where the old and new positions differ by $\sim 10''$, a discrepancy already pointed out by Wolf-Chase et al. (1998). All these objects are detected in our observations. In addition, we identified 21 new discrete sources with peak flux densities above the $\sim 4.5\sigma$ level of 4.0 mJy/beam. We are confident that this is an appropriate threshold since all our detected sources in the S68N/SMM1 region are "visible", but at lower confidence level, in the lower resolution SCUBA observations at 450 μm (Wolf-Chase et al. 1998) and in BIMA/IRAM-30m observations at 3 and 1.3 mm (Williams et al. in preparation).

We calculated the mass of each of the sources of emission assuming optically thin dust thermal emission, with $M_d = S_\nu\, D^2/(\kappa_\nu\, B_\nu(T))$, where S_ν is the observed integrated flux density, D is the distance from the Sun, $B_\nu(T)$ is the Planck function at the assumed dust temperature T, and κ_ν is the dust mass opacity coefficient. We assumed $T = 15$ K and $\kappa_\nu = \kappa_{230GHz}(\nu/230GHz)^\beta$. Following Preibish et al. (1993), we adopted $\kappa_{230GHz} = 0.005$ cm^2 g^{-1}, assuming a gas to dust ratio of 100 by mass. This value of κ_{230GHz} is consistent with recent measurement in the cold cloud core IC 5146 (Kramer et al. 1998a), and agrees to within a factor of two with that derived for the envelopes around young stellar objects, ~ 0.01 cm^2 g^{-1} by Ossenkopf & Henning (1994). We derived approximate values for β by fitting a power law of the form $F_\nu \sim \nu^{\beta+2}$ to our 3 mm flux and the sub-mm measurements of CED, for each of our six common sources. These fits are shown as dotted lines in Fig. 2. In general the OVRO point is consistent with the single dish fluxes, indicating that the sources are compact and that there is no significant missing flux from spatially extended envelopes. Values of β range from 0.7 to 1.6, and we adopted a mean of 1.1 for all the sources in our map. Our detection limit of 4.0 mJy/beam then correnspponds to a mass ~ 0.4 M$_\odot$ and, assuming a mean molecular weight of 2.33, a beam-averaged H_2 column density of $\sim 3 \times 10^{23}$ cm^{-2}. The mass of each of the clumps and our mass detection limit depend on the adopted parameter values. Nevertheless, as long as the emission is optically thin and all clumps have similar temperatures and opacities, the *shape* of the mass function is independent of the particular values assumed.

We assume that the mm-sources are a collection of prestellar condensations, collapsing protostars or circumstellar structures around more evolved objects, all of which are expected to show significant continuum emission at mm wavelengths (e.g. Shu et al. 1987; André 1996). A spherical, isothermal gas cloud with a radius of 2000 AU, a temperature of 15 K and supported by thermal pressure is gravitationally bound if it is more massive than ~ 0.3 M$_\odot$ (e.g. Bonnor 1956). Given that 2000 AU is the upper radius for detected

sources and ~ 0.4 $M_\odot$ the lower mass limit, all the clumps are likely to be bound. To ensure that the mass function for condensations (clumps) that will eventually produce stars is not contaminated by young stellar objects, we checked for counterparts to our 3 mm sources in the near infrared (NIR) observations of Giovannetti et al. (1998) and the 12 μm detections by Hurt & Barsony (1996). Only two 12 μm sources, PS1 and PS2, and 4 additional NIR sources (which include the two NIR sources associated with SMM5 and SMM6) could be considered possible associations; we discarded these 6 sources from our list. According to the arguments presented by André (1996), the lack of infrared detections suggests that all other clumps, $\sim 80\%$ of the total, are either prestellar or protostellar in nature. This is a much larger fraction than found in ρ-Oph by Motte et al. (1998); their higher mass sensitivity limit enables an increased detection rate for faint circumstellar material around young stars.

In Fig. 3 the mass spectrum and the cumulative mass function of the remaining mm sources are shown. The best fitting power law, $dN/dM \sim M^{-2.1}$, is represented by a dotted line. That corresponding to the Salpeter (1955) local IMF, $dN/dM \sim M^{-2.35}$, is a dashed line while the -1.7 power–law spectrum of gaseous clumps is a dot-dashed line (Kramer et al. 1998b; Williams, Blitz & McKee 1998). Our data are too scant to be compared with the field stars IMF derived by Kroupa et al. (1993). Nevertheless, our fitted power law index is very close to their $a_2 = 2.2$ index for solar and slightly subsolar masses and we view the agreement between the observed mass spectrum for the clumps and the stellar mass function for the field stars as very promising. The cumulative mass function for the clumps, which does not rely on data binning, provides a more robust comparison; the -1.7 power–law is rejected by the Kolmogorov-Smirnov test at the 98% confidence level.

4. Implications

Our results indicate that the mass spectrum of the protostellar dust condensations in the Serpens core closely resembles the local IMF. A similar result was found for condensations in the ρ Oph cloud core (Motte et al. 1998). With $dN/dM \sim M^{-2.1}$, the slope of the clump mass spectrum is substantially steeper than that derived for gaseous clumps. This strongly suggests that the stellar IMF results from the fragmentation process in turbulent cloud cores, rather than from stellar accretion mechanisms. In fact, the observed 3 mm continuum clumps may be the direct descendants of the "kernels" discussed by Myers (1998) that have evolved through gravitational contraction. In Fig. 1, the typical distance between discrete sources is ~ 0.03–0.06 pc, the typical size of Myers' kernels.

Our conclusions are, of course, preliminary. More definitive statements must await the

completion of high resolution surveys of a substantial number of cores. The remarkable agreement between the clump mass function and the stellar IMF must also be viewed with caution. A small fraction of our surveyed area has not been observed in the near infrared survey of Giovannetti et al. (1998), and high resolution, high sensitivity measurements of the whole region in the mid- to far-infrared are critical to identifying and eliminating all young stellar objects from our sample. Nevertheless, our results show that high resolution, millimeter wave observations of relatively large star forming areas coupled with near- and mid-infrared surveys, provide an excellent way to constrain the origin of the IMF in cluster-forming cloud cores.

Acknowledgements: We thank Francesco Palla, Jonathan Williams, John Carpenter and an anonymous referee for useful discussions and constructive criticism. The Owens Valley millimeter-wave array is supported by NSF grant AST-96-13717. Funding from the C.N.R.–N.A.T.O. Advanced Fellowship program and from NASA's *Origins of Solar Systems* program (through grant NAGW–4030) is gratefully acknowledged. Research at Owens Valley on the formation of young stars and planets is also supported by the *Norris Planetary Origins Project*.

REFERENCES

Adams, F. C. & Fatuzzo, M. 1996, ApJ, 464, 256

André, P. 1996, Mem. SAIt, 67, 901

Bonnor, W. B. 1956, MNRAS, 116, 351

Casali, M. M., Eiroa, C., & Duncan, W. D. 1993, A&A, 275, 195, CED

Eiroa, C., & Casali, M. M. 1992, A&A, 262, 468

Giovannetti, P., Caux, E., Nadeau, D., & Monin, J.-L. 1998, A&A, 330, 990

Hillenbrand, L. A. 1997, AJ, 113, 1733

Hurt, R. L., & Barsony, M. 1996, ApJ, 460, L45

Kitamura, Y., Kawabe, R., & Ishiguro, M. 1992, PASJ, 44, 407

Klessen, R. S., Burkert, A., & Bate, M. R. 1998, ApJ, 501, L205

Kramer, C., Alves, J., Lada, C., Lada, E., Ungerechts, H., Walmsley, C. M. 1998a, A&A, 329, L33

Kramer, C., Stutzki, J., Röhring, R., & Corneliussen, U. 1998b, A&A, 329, 249

Kroupa, P., Tout, C. A., & Gilmore, G. 1993, MNRAS, 262, 545

Lada, C. J., Alves, J., & Lada, E. A. 1996, AJ, 111, 1964

Lada, E. A. 1992, ApJ, 393, L25

de Lara, E., Chavarria–K., C., & López–Molina, G. 1991, A&A, 243, 139

Loren, R. B., Evans, N. J., II, & Knapp, G. R. 1979, ApJ, 234, 932

McMullin, J. P., Mundy, L. G., Wilking, B. A., Hezel, T., & Blake, G. A. 1994, ApJ, 424, 222

Motte, F., André, P., & Neri, R. 1998, A&A, 336, 150

Myers, P. C. 1998, ApJ, 496, L109

Ossenkopf, V., & Henning, Th. 1994, A&A, 291, 943

Pratap, P., Batrla, W., & Snyder, L. E. 1990, ApJ, 351, 530

Preibisch, Th., Ossenkopf, V., Yorke, H. W., & Henning, Th. 1993, A&A, 279, 577

Salpeter, E. E. 1955, ApJ, 121, 161

Scoville, N. Z., Carlstrom, J. E., Chandler, C. J., Phillips, J. A., Scott, S. L., Tilanus, R. P. J., & Wang, Z. 1993, PASP, 105, 1482

Shu, F. H., Adams, F. C., & Lizano S. 1987, ARAA, 25, 23

Strom, S. E., Grasdalen, G. L., & Strom, K. M. 1974, ApJ, 191, 111

Testi, L., Palla, F., & Natta, A. 1998, A&A, submitted

Ungerechts, H. & Güsten, R. 1984, A&A, 131, 177

Williams, J., Blitz, L., & McKee, C. 1998, in Protostars & Planets IV, ed. V. Mannings, A. Boss & S. Russel (Tucson: Univ. Arizona Press), in press

White, G. J., Casali, M. M., & Eiroa, C. 1995, A&A, 298, 594

Wolf-Chase, G. A., Barsony, M., Wootten, H. A., Ward-Thompson, D., Lowrance, P. J., Kastner, J. H., & McMullin, J. P. 1998, ApJ, 501, L193

Zinnecker, H., McCaughrean, M. J., & Wilking, B. A. 1993, in Protostars & Planets III, ed. E. Levy & J. I. Lunine (Tucson: Univ. Arizona Press), 429

This preprint was prepared with the AAS LaTeX macros v4.0.

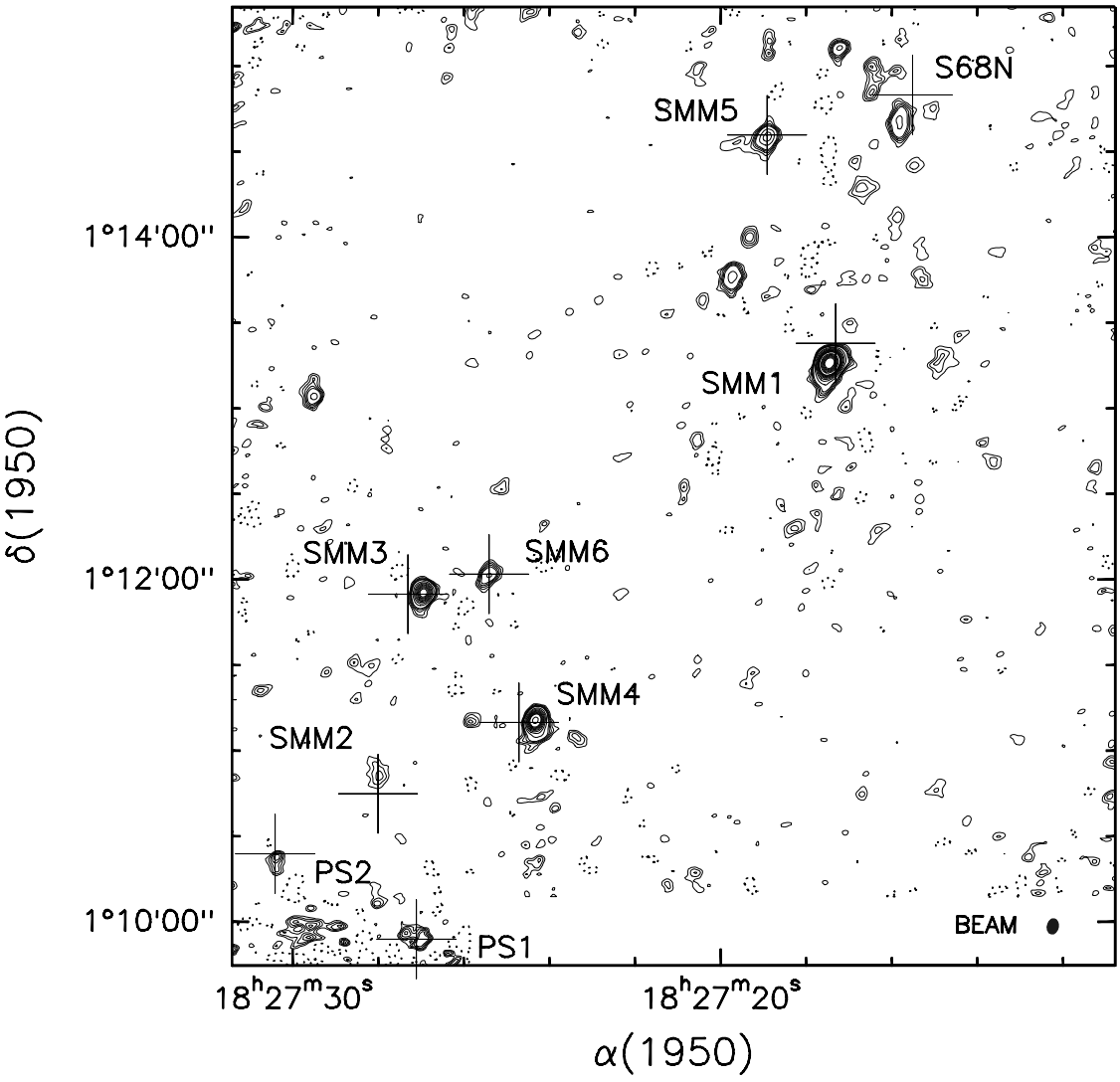

Fig. 1.— OVRO 3 mm continuum mosaic of the Serpens core. Contour levels are −2.7, 2.7 to 6.3 by 0.9, 10 to 42 by 4, 55 to 105 by 10 mJy/beam. The positions of the known sub-millimeter sources (CED) and far-infrared sources (Hurt & Barsony 1996) are marked by crosses. Note that we detect all the sources already identified and have refined the positional accuracy. In addition, numerous new sources can be seen. The synthesized beam, $5\farcs5 \times 4\farcs3$ (FWHM), is shown as a filled ellipse in the lower right corner.

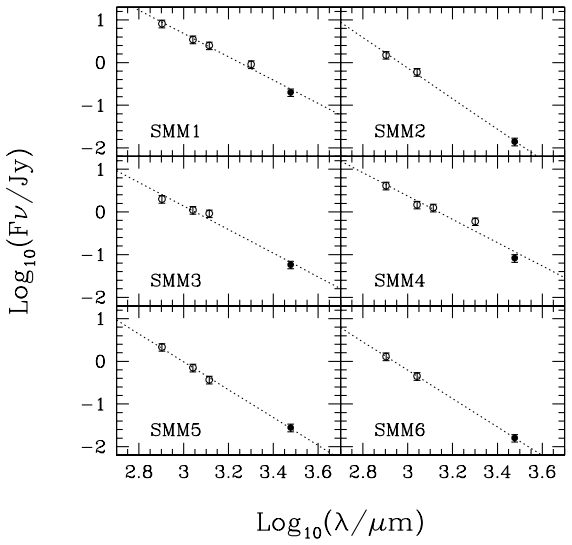

Fig. 2.— Continuum spectra for the 6 sources in common with CED; open circles: their JCMT measurements; filled circles: OVRO 3 mm fluxes. For each source, a power law spectrum has been fitted assuming $F_\nu \sim \nu^{\beta+2}$.

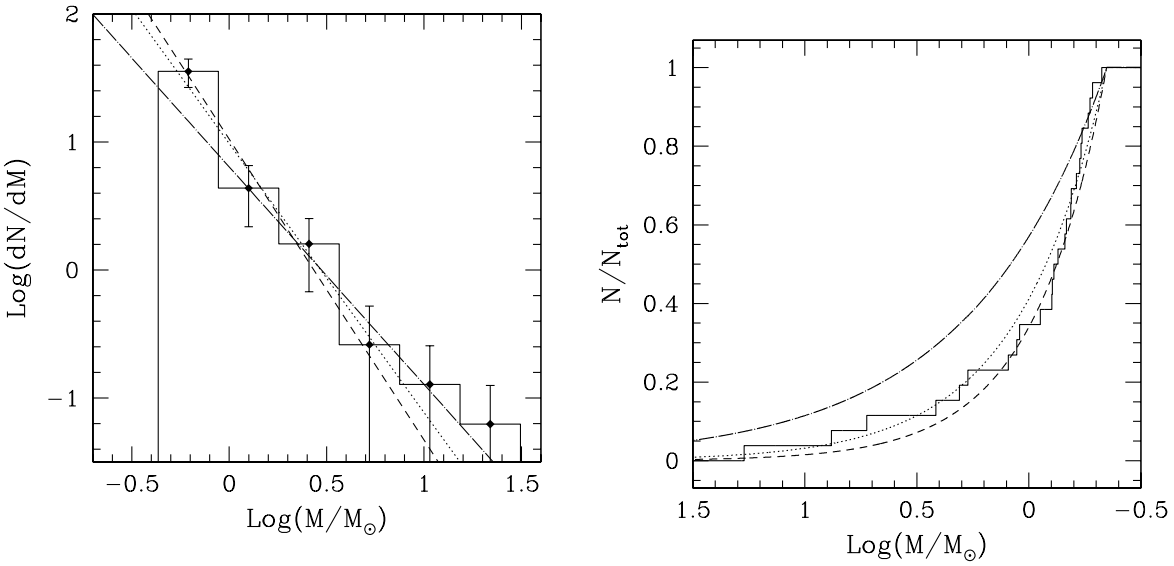

Fig. 3.— Left: the mass spectrum for the 3mm continuum sources. The dotted line is the best fitting power law, dN/dM$\sim$M$^{-2.1}$; the dashed line represents the Salpeter IMF, dN/dM$\sim$M$^{-2.35}$; the dot-dashed line is a -1.7 power–law. Right: the normalized cumulative mass distribution. Dotted, dashed and dot-dashed lines are as on the left panel.